PHYSICAL REVIEW B **76**, 140504(R) (2007)

Properties of high-T_C copper oxides from the nearly-free-electron model

T. Jarlborg
DPMC, University of Geneva, 24 Quai Ernest-Ansermet, CH-1211 Geneva 4, Switzerland
(Received 14 August 2007; revised manuscript received 24 September 2007; published 15 October 2007)

The generic band structure of high-T_C copper oxides is simulated by the nearly-free-electron model in two dimensions with parameters from *ab-initio* linear muffin-tin orbital calculations. Interaction between phonons and spin waves will cause potential modulations, and pseudogaps and the strength of the modulations, the wavelengths, and the doping are all related. A Fermi-surface "arc" is found for dynamic spin and phonon waves. The confinement of superconductivity between two limiting dopings can be a result of competition with the pseudogap at low doping and weak coupling at high doping.

DOI: 10.1103/PhysRevB.76.140504 PACS number(s): 74.20.−z, 71.10.−w, 74.72.−h

An important structural feature of high-T_C materials is the stacking of almost two-dimensional (2D) CuO planes. All high-T_C cuprates have at least one of these layers in the unit cell, and they make the band structure fairly simple with one or more M-centered Fermi surface (FS) cylinders. Band calculations and photoemission agree essentially on this fact, except for details and for undoped materials, which often are antiferromagnetic (AFM) insulators.[1] The density of states (DOS) at the Fermi energy (E_F) is mainly of Cu d character with some O p admixture. The views on the mechanism for superconductivity and normal-state properties diverge. Extensive experimental works show that not only the high T_C, but also many normal-state properties, are unusual. These include pseudogaps and magnetic fluctuations, both with rich dependences as a function of doping x and temperature T. The importance of phonons is evidenced by isotope effects on T_C and pseudogaps,[2,3] and magnetic fluctuations are detected by neutron scattering.[4]

Here is presented a nearly-free-electron (NFE) model for high-T_C properties with use of parameters coming from *ab initio* linear muffin-tin orbital[5] (LMTO) band calculations in the local spin-density approximation[6] (LSDA) for pure and hole-doped high-T_C materials.[7,8] Lattice distortions within long supercells are used to model phonons, and spin-polarized calculations, which include staggered magnetic fields on the Cu sites in the cells, are used to study the behavior of spin waves. These band calculations show important coupling between phonon and spin waves. The difficulty with *ab initio* calculations is that a unit cell with interesting phonon displacements and/or spin waves needs to be very large. In addition, the bands are not obtained within the normal Brillouin zone (BZ), but within the down-folded zone. Such calculations are so far limited to spin waves and phonons along one direction only ("1D-LMTO"), while in reality one can expect modulations along $\hat{x}$ and $\hat{y}$ (checkerboard modulations rather than stripes). The qualitative results from the (1D) NFE model and LMTO calculations are the same, and it is worthwhile to extend the NFE model to 2D.

A periodic potential perturbation $V(\vec{x})=V_Q \exp(-i\bar{Q}\cdot\vec{x})$ will open a gap of size $2V_Q$ at the zone boundary, $\bar{k}=\bar{Q}/2$, in the 1D NFE bands.[9,10] This well-known NFE result can be applied to the AFM spin arrangement on neighboring Cu along [1,0,0] (with wave vector Q) in undoped insulating cuprates. An additional modulation, with wave vector $\bar{q}<\bar{Q}$, modifies the potential, $V(\vec{x})=V_Q \exp(-i\bar{Q}\cdot\vec{x})\exp(i\bar{q}\cdot\vec{x})$. The gap moves away from $\bar{Q}/2$ to $(\bar{Q}-\bar{q})/2$, as for in LMTO for supercells of different lengths. The combined potential modulation leads to stripelike phonon or spin-wave patterns, with short wavelengths (periodicity, with wave vector $\vec{q}$) at high doping and long ones when $x\rightarrow 0$, as from the LMTO results.[8]

Simultaneous modulations along $\hat{x}$ and $\hat{y}$ are yet too difficult for LMTO calculations, at least for realistic wavelengths. An extension of the NFE model for potential modulations along $\hat{x}$ and $\hat{y}$ leads to a 3×3 eigenvalue problem of the form $E-k_x^2-k_y^2$, $E-(k_x-Q_x)^2-k_y^2$, and $E-k_x^2-(k_y-Q_y)^2$ in the diagonal and V_Q as nondiagonal terms. The G vectors 0, $\bar{Q}_x=\bar{Q}-\overline{q_x}$, and $\bar{Q}_y=\bar{Q}-\overline{q_y}$ are considered in the basis with $\overline{q_x}$ and q_y along $\hat{x}$ and $\hat{y}$. The bands are represented in the reduced zone as for the normal unit cell. The band width from the Γ point up to $\hat{k}_F$ is about 0.125 Ry when V_Q, q_x, q_y, and x are all zero and the effective mass is 1.3. The position of the Van Hove singularity (when the bands touch X and Y) corresponds to $x\approx 0.2$. Potential modulations will open gaps near X and Y, while not much happens between Γ and M.[8]

Superconductivity and pseudogaps appear typically at 100 K, and we will estimate the V_Q parameters for this temperature. The mean value of atomic displacements $u=\sqrt{(3k_BT/K)}$, where the force constant (K) for O vibrations is of the order of 25 eV/Å^2 for $\hbar\omega\approx 50$ meV, is close to $0.01a_0$, where a_0 is the lattice constant. Zero-point motion is just a bit larger, but it is not selective to one phonon.[11] The mean value of magnetic moment fluctuations, m_0, is obtained through $k_BT=\frac{1}{2}Fm^2$, where $F=d^2E/dm^2$ and E is the total energy. For a short spin-phonon wave in $HgBa_2CuO_4$,[7] V_Q^{sf} is about 6 mRy for $m_0\sim 0.09\mu_B$ per Cu.

The origin of V_Q is two fold. Structural distortions of phononic origin contribute equally to the two spin components of $V(\vec{x})$, while for a spin wave there is an opposite phase of the two spin potentials. A static spin-polarized modulation of the potential determines AFM order in the undoped case. Phonons, and probably also long-wave spin modulations, are dynamic. From the LMTO for "half-breathing" phonons along [1,0,0] it is estimated that V_Q^{ph} varies from 5 to 11 mRy when the wavelength varies from $4a_0$ to $16a_0$. This is when the atomic displacement is of the order of $0.01a_0$, as when $T\approx 100$ K.[8] The phonon amplifies a spin

TABLE I. Spin density coefficients $[A\cos^2(\pi x/2)$ and $B\sin^2(\pi x/2)]$ for the NFE state below the gap at the zone boundary along q_x. The exchange splitting for spin fluctuations, V_Q^{sf}, is estimated from the scaling procedure as described in the text. The last column shows the potential parameter for phonons, V_Q^{ph}, which are interpolated from band results for $Q \leqslant 0.9$. A saturation is assumed for $Q \geqslant 0.9$.

Q_x	Q_y	$(A-B)$	V_Q^{sf} (mRy)	V_Q^{ph} (mRy)
0.99	0.99	0.98	32	12
0.95	0.95	0.70	22	12
0.90	0.90	0.47	15	11
0.83	0.83	0.33	11	9
0.75	0.75	0.25	8	9
0.50	0.50	0.18	6	7
0.75	0.85	0.25	7	9
0.75	0.95	0.25	6	9

wave, which has twice as long a wavelength as the phonon. But the two types of waves enforce a common gap at the same energy, and some increase of V_Q^{ph} can come from mutual coupling.[12]

The self-consistent LMTO converges very slowly for long-wave spin configurations. In order to estimate the spin-polarized part V_Q^{sf} we rely on the band results for a short spin wave and do NFE scaling for longer waves. Band calculations on undoped $Hg_2Ba_4Cu_2O_8$ show that an AFM, zero-gap state can be stabilized with a spin splitting of 23 mRy on Cu.[7] (Larger gaps are possible when using a different density functional in band calculations for La_2CuO_4.[13]) This determines the V_Q^{sf} for the basic AFM spin arrangement between nearest Cu neighbors. A well-known feature of the 1D NFE model is the spatial separation of the states below the gap $[\Psi_-^2(\hat{x})=\sin^2(Gx/2)]$ and above the gap $[\Psi_+^2(\hat{x})=\cos^2(Gx/2)]$.[9] Let the state below (above) the gap coincide with the Cu with the attractive (repulsive) potential for one spin. The spin density of the first (second) spin is given by the $\sin^2$ ($\cos^2$) term, and the phase on the nearest Cu neighbor differs by π. The densities feed the exchange splitting of the potentials. If they diminish, it leads to a smaller exchange, which leads to smaller densities and so on, in a self-consistent manner. Thus, the spin density is a driving force behind the near-neighbor AFM configuration and it depends on the optimal occupation of the two states.

An additional modulation will reduce the spatial separation of the two states at $G/2$, as shown by the coefficients $(A-B)$ in Table I for different $\vec{Q}_x$. As V_Q^{sf} depends on the near-neighbor interaction, one can expect a reduction of V_Q^{sf} through these coefficients. This does not include self-consistent feedback or the closing of the pseudogap at T^* (see later), effects which both should decrease V_Q^{sf}. On the other hand, V_Q^{sf} is enhanced by coupling to phonons for all $\vec{q}>0$. The moments from LMTO calculations are enhanced by ~32% and ~35%, when the spin waves (with Q_x equal to 0.5 and 0.75, respectively) coexist with phonon distortions of the appropriate u. The V_Q^{sf} in Table I are estimated as $23(A-B)f$, where f is the "phonon enhancement" factor (extrapolated from 1.32 to 1.38 for Q between 0.5 and 0.99) and 23 (mRy) is the exchange for $Q=1$ (without phonon) from LMTO calculations. Usually T^* is well above the 100 K at which the parameters are estimated. But when T^* goes to zero at large doping, it will reduce V_Q^{sf} more because the Fermi-Dirac (FD) occupation will mix the states across the pseudogap. Thus, the V_Q^{sf} in the two last lines of the table are reduced further by rather arbitrary reduction factors of 0.9 and 0.8, since $T^* \rightarrow 100$ K. All these estimates are approximate, but it can be recalled that V_Q^{sf} at $q_x=q_y=0.5$ from the rescaling, 6 mRy, agree well with the best converged 1D-LMTO result for the spin wave $(4a_0)$ in doped $HgBa_2CuO_4$.[7]

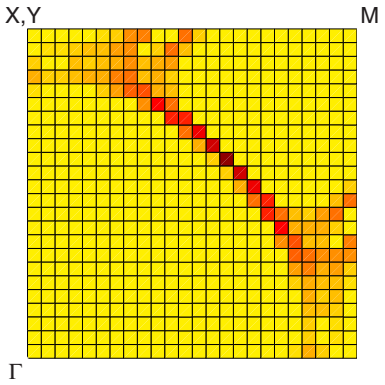

FIG. 1. (Color online) Calculated 2D NFE Fermi surface for a strong dynamic spin-phonon fluctuation with $\vec{q}=(0.85,0.90)$.

An example of the FS is shown in Fig. 1, which is a sum of several calculations with V_Q ranging from 10 to 30 mRy in order to simulate dynamical waves. The position of E_F is chosen at the minimum of the sum of the partial DOS functions, and the plot is finally symmetrized along the Γ-M line. The FS remains as a sharp "arc" in the diagonal direction, while it is washed out near the limits of the zone because of the fluctuations of V_Q. The result is compatible with the observation of a small section of a FS arc at low T.[14] The arc widens for larger T, when most of the potential modulations and the pseudogap are gone. Static potential modulations will bend the outer sections of the FS towards the X,Y-M lines,[8] which in a repeated zone looks like a second "ghost band."

Calculations of the DOS (Fig. 2) and the relation between doping and q vectors (Fig. 3) are made using $V_Q=V_Q^{sf}+V_Q^{ph}$ from Table I as input. The Q vectors are allowed to vary from 1.0 to 0.75 in the $\hat{x}$ and $\hat{y}$ directions, and the doping is optimal when E_F coincides with the energy at the DOS minimum, at the pseudogap. Three examples of doping are shown in Fig. 2. At low doping ($x \leqslant 0.18$) there is a nearly linear relation between x and q (see Fig. 3), and the Q vectors along $\hat{x}$ and $\hat{y}$ have equal lengths down to the minimum at 0.75 of the zone boundary limit. There is no possiblity to obtain a minimum in the DOS for larger doping with equal $|\vec{Q}_x|$ and $|\vec{Q}_y|$; the values of V_Q are too small. However, if one of the Q vectors remains fixed at the value 0.75 (assumed to correspond to the shortest possible magnetic modulation[4]) while the other one increases, it is possible to follow the pseudogap further towards large x, with V_Q coming from Table I. [The larger of the two Q vectors makes a dip in the

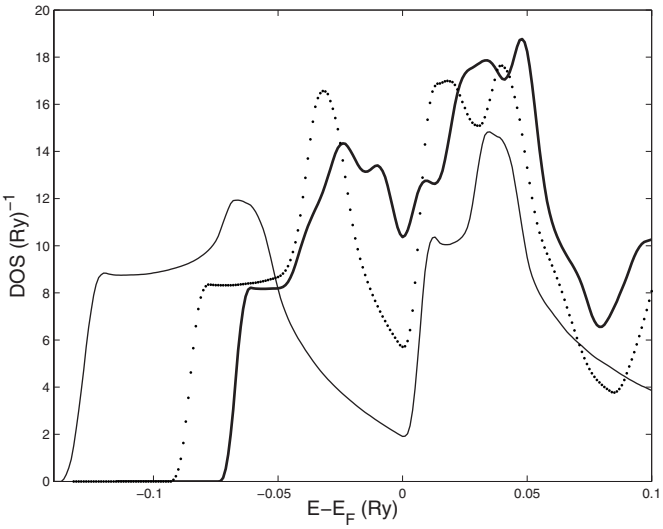

FIG. 2. Calculated DOS for $x=0.02$ (thin line), $x=0.16$ (dotted line), and $x=0.26$ (heavy line). The latter case is for nonequivalent modulations along $\hat{x}$ and $\hat{y}$, and a secondary dip below E_F is seen.

DOS, but it is weak and below E_F (see Fig. 2), so its modulation should be harder to detect.] The result in Fig. 3 is qualitatively similar to the doping dependence observed in $La_{(2-x)}Sr_xCuO_4$ by Yamada *et al.*,[15] although saturation of the periodicity occurs near $x\sim 0.18$ compared to about 0.12 as observed. Other combinations of Q vectors and V_Q can give larger x, but with weaker gaps or unrealistic values of V_Q.

The unperturbed NFE band is perfectly isotropic, but the real band structure may have different dispersion in different directions. A FS which extends more towards the diagonal than towards X and Y can be modeled by an anisotropic effective mass. Here, through multiplication of the mass with $[(|k_x|+|k_y|)/(|k_x+k_y|)]^{1/3}$ we test a $\sim$10% anisotropy. The result is that the scale of the doping in Figs. 3 and 4 becomes

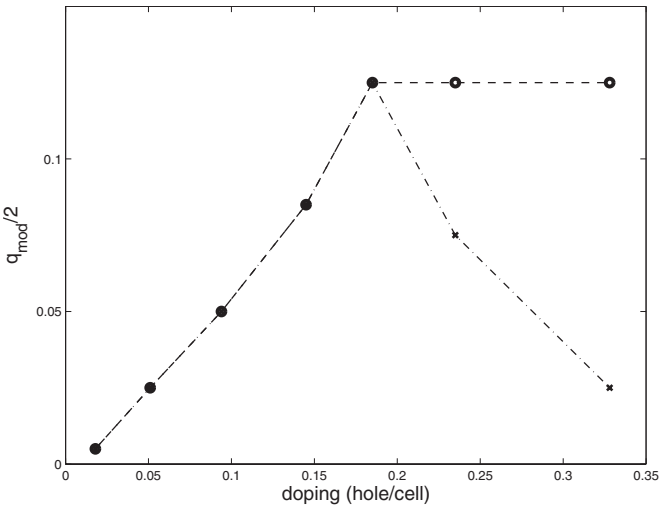

FIG. 3. The relation between doping x and q vectors of the modulation. The q vectors along $\hat{x}$ and $\hat{y}$ are equal for doping below $\sim$0.18. The modulation along one direction remains fixed ($8a_0$ for the spin part) for larger doping, with a weaker modulation of longer periodicity in the perpendicular direction.

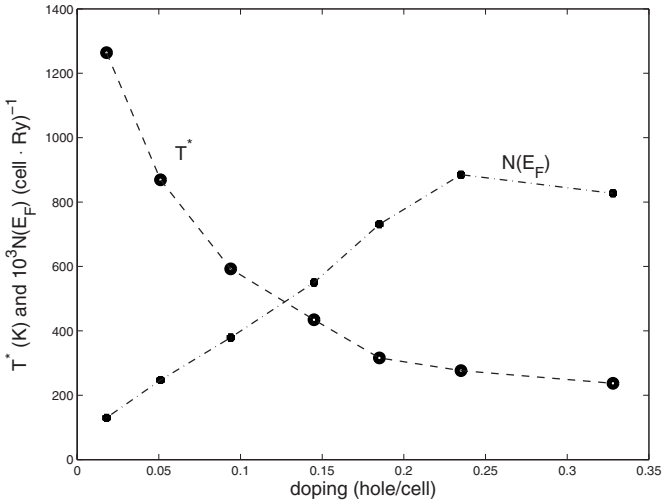

FIG. 4. The DOS at E_F and T^* as function of doping x. The DOS is at the minimum of the pseudogap, and T^* is 1/4th of V_Q^{sf}.

compressed, and the breaking point in Fig. 3 is at $x=0.13$ instead of at 0.18, which would fit better to the results by Yamada *et al.*[15] The values of $N(E_F)$ will go down slightly, especially for small x. This shows that details of the real band structure can be important for the quantitative results. LMTO bands in undoped $HgBa_2CuO_4$ (Ref. 10) suggest that the FS retracts towards the diagonal.

The relation between doping and wavelength from the 1D-LMTO for long supercells appears to be very exact. For instance, a doubling of a cell will result precisely to a factor of 2 in the doping. This is because practically all E_k (near E_F) in the compressed 1D BZ become gapped. Many states in the interior of the zone in the 2D NFE model are not concerned by gaps. All states contribute to the DOS and the energies of local gaps do not correspond to the pseudogap in the total DOS. One could return to the more "exact" relation if the 2D sheet of the NFE band behaved very rigidly with similar gaps everywhere.

The T-dependent FD occupation leads to a quenching of the spin wave by the feedback of the spin density onto the potential. The quenching temperature defines T^*, which in a 1D model is about $\frac{1}{4}\Delta/k_B$, where $\Delta\approx V_Q^{sf}$ is the gap at $T=0$.[8] Figure 4 shows T^* and $N(E_F)$ as a function of the doping from the model.

The change of $\vec{q}$ as function of coupling strength was not forseen in the 1D-LMTO results. If it is true, then one can expect longer wavelength for weaker coupling, near T^*, for instance. This implies that the gap moves away from E_F, which is less favorable for the stability of the wave, and the process of quenching at T^* may accelerate. The same mechanism predicts isotope shifts on the q vectors of magnetic fluctuations, since a heavier mass is expected to decrease V_Q^{sf} through smaller u.[8,16]

The LMTO calculations for a phonon and a spin wave along [1,0,0], which differ by a factor of 2 in wavelength, tend to open a gap at the same energy. However, the spatial shape of the potential perturbation caused by a phonon and a spin wave is different (this is less clear from the NFE model) and regarding superconductivity it is not expected that the

V_Q's of the two waves work together. The spin wave and equal-spin pairing (ESP) are probably most important for superconductivity, since V_Q^{sf} can become very large, as when a favorable phonon displacement is assisting. These arguments suggest ESP as a mechanism for superconductivity, but it has to compete with the pseudogap which removes states and DOS near E_F, more so at low doping (see Fig. 4). This scenario is corroborated by recent femtosecond spectroscopic measurements on cuprates showing competing order from something like a pseudogap within the superconducting gap.[17] The coupling for spin fluctuations decreases towards the overdoped side, as is reflected by the decreasing V_Q^{sf} values in Table I. Also the coupling to phonons disappears at too short wavelengths, since no spin wave shorter than $4a_0$ can coexist with a "half-breathing" phonon. The coupling parameter $\lambda \sim NV^2$ and T_C will therefore vanish at the extreme dopings, as can be deduced from Fig. 4 by the low DOS for $x \rightarrow 0$ and the small T^* (which is proportional to V_Q^{sf}) at large doping. The present results are not sufficiently complete for an evaluation of T_C through a BCS-like formula, but qualitatively it is expected that the limits of a "T_C dome" are shaped by the lines for T^* and $N(E_F)$, as in Fig. 4. In order to increase T_C on the underdoped side one should increase $N(E_F)$. One possiblity is to make the 2D sheet of the band less rigid in order to restrict the gaps to the exterior of the BZ, perhaps by pressure.

Many typical high-T_C features, such as FS arcs, pseudogaps, T^*, and the $q(x)$ dependence, can be described qualitatively by NFE simulations. The total V_Q determines the size of the pseudogap, but V_Q^{sf} disappears above T^* and the same gap cannot be supported by V_Q^{ph} alone. The smaller V_Q^{ph} makes a weak dip in the DOS at lower energy, away from E_F and away from optimal doping. It is suggested that superconductivity is caused by ESP and V_Q^{sf}, which leads to confinement of T_C between two limiting dopings. The parameters are based on previous LMTO calculations for phonons and spin waves in doped systems, and the values in Table I are the most probable V_Q to use in the 2D-NFE model. Still, it is unavoidable that some of the estimations are very uncertain. But finally, the extreme simplicity of the 2D NFE model makes it a toy model, where other solutions of the parameter space can be tested.

I am grateful to B. Barbiellini and C. Berthod for various discussions.

[1] A. Damascelli, Z.-X. Shen, and Z. Hussain, Rev. Mod. Phys. **75**, 473 (2003) and references therein.
[2] R. Khasanov, A. Shengelaya, E. Morenzoni, K. Conder, I. M. Savic, and H. Keller, J. Phys.: Condens. Matter **16**, S4439 (2004).
[3] G.-H. Gweon, T. Sasagawa, S. Y. Zhou, J. Graf, H. Takagi, D.-H. Lee, and A. Lanzara, Nature (London) **430**, 187 (2004).
[4] J. M. Tranquada, e-print arXiv:cond-mat/0512115 and references therein.
[5] O. K. Andersen, Phys. Rev. B **12**, 3060 (1975); T. Jarlborg and G. Arbman, J. Phys. F: Met. Phys. **7**, 1635 (1977).
[6] W. Kohn and L. J. Sham, Phys. Rev. **140**, A1133 (1965); O. Gunnarson and B. I. Lundqvist, Phys. Rev. B **13**, 4274 (1976).
[7] T. Jarlborg, J. Phys.: Condens. Matter **16**, L173 (2004).
[8] T. Jarlborg, Physica C **454**, 5 (2007).
[9] J. M. Ziman, *Principles of the Theory of Solids* (Cambridge University Press, New York, 1971).
[10] T. Jarlborg, Phys. Rev. B **64**, 060507(R) (2001).
[11] G. Grimvall, in *Thermophysical Properties of Materials*, edited by E. P. Wohlfarth (North-Holland, Amsterdam, 1986).
[12] T. Jarlborg, Phys. Lett. A **295**, 154 (2002).
[13] J. K. Perry, J. Tahir-Kheli, and W. A. Goddard III, Phys. Rev. B **65**, 144501 (2002).
[14] M. R. Norman, H. Ding, M. Randeria, J. C. Campuzano, T. Yokoya, T. Takeuchi, T. Takahashi, T. Mochiku, K. Kadowaki, P. Guptasarma, and D. G. Hinks, Nature (London) **392**, 157 (1998).
[15] K. Yamada, C. H. Lee, K. Kurahashi, J. Wada, S. Wakimoto, S. Ueki, H. Kimura, Y. Endoh, S. Hosoya, G. Shirane, R. J. Birgeneau, M. Greven, M. A. Kastner, and Y. J. Kim, Phys. Rev. B **57**, 6165 (1998).
[16] T. Jarlborg, Phys. Rev. B **68**, 172501 (2003).
[17] E. Chia, J.-X. Zhu, J. Talbayev, R. D. Averitt, K.-H. Oh, I.-S. Jo, S.-I. Lee, and A. J. Taylor, arXiv:0705.1724.